Published in final edited form as:
Curr Biol. 2001 May 1; 11(9): 671–683.

The schedule of destruction of three mitotic cyclins can dictate the timing of events during exit from mitosis

Devin H. Parry and **Patrick H. O'Farrell**
Department of Biochemistry and Biophysics, University of California, San Francisco, San Francisco, California, 94143

Abstract

Background—Degradation of the mitotic cyclins is a hallmark of the exit from mitosis. Induction of stable versions of each of the three mitotic cyclins of *Drosophila*, cyclins A, B, and B3, arrests mitosis with different phenotypes. We tested a recent proposal that the destruction of the different cyclins guides progress through mitosis.

Results—Real-time imaging revealed that arrest phenotypes differ because each stable cyclin affects specific mitotic events differently. Stable cyclin A prolonged or blocked chromosome disjunction, leading to metaphase arrest. Stable cyclin B allowed the transition to anaphase, but anaphase A chromosome movements were slowed, anaphase B spindle elongation did not occur, and the monooriented disjoined chromosomes began to oscillate between the spindle poles. Stable cyclin B3 prevented normal spindle maturation and blocked major mitotic exit events such as chromosome decondensation but nonetheless allowed chromosome disjunction, anaphase B, and formation of a cytokinetic furrow, which split the spindle.

Conclusions—We conclude that degradation of distinct mitotic cyclins is required to transit specific steps of mitosis: cyclin A degradation facilitates chromosome disjunction, cyclin B destruction is required for anaphase B and cytokinesis and for directional stability of univalent chromosome movements, and cyclin B3 degradation is required for proper spindle reorganization and restoration of the interphase nucleus. We suggest that the schedule of degradation of cyclin A, cyclin B, and then cyclin B3 contributes to the temporal coordination of mitotic events.

Background

Mitosis includes events of sweeping scope, such as remodeling of the cytoskeleton to construct a spindle, sister chromosome disjunction, spindle elongation, and cytokinetic furrow formation. The extraordinary reliability of mitotic segregation relies on the precise coordination of these events. Despite advances in understanding cell cycle control, we have only a bare outline of the circuits that control and coordinate the myriad events of mitosis. Two central components of the cell cycle machinery have been shown to govern aspects of mitosis, the mitosis promoting factor (MPF), which consists of an activated complex of cyclin and a cyclin dependent protein kinase (Cdk), and the anaphase promoting complex (APC), an elaborate E3 complex that ubiquitinates key mitotic regulators and promotes their degradation [1,2].

Correspondence: Patrick H. O'Farrell: ofarrell@cgl.ucsf.edu.

Supplementary material
The real-time movies described in the text that illustrate the phenotypes of the different stable cyclin arrests can be found with the electronic version of this article at http://images.cellpress.com/supmat/supmatin.htm.

Early ideas for the control of mitosis had appealing simplicity. MPF (cyclin/Cdk) was thought to promote entry into mitosis, leading to alignment of the chromosomes at metaphase, and APC was thought to promote anaphase and exit from mitosis by triggering the destruction of cyclins and MPF inactivation. Genetic and biochemical studies of cyclins and Cdks confirmed their contribution to the promotion of mitosis [1]. The inferred role of cyclin destruction in the exit from mitosis was supported by the production of mutant forms of cyclin lacking the destruction box sequence recognized by the APC. Expression of such stable cyclins in species ranging from yeast to human arrested cells in mitosis [3–10]. Thus, an on-off model of cyclin/Cdk regulation could explain alternation between mitotic and interphase states, but it did not explain control of events within mitosis. Importantly, efforts to understand the control of one such event, the metaphase/anaphase transition, challenged the adequacy of this model.

In a key analysis, Holloway et al. examined the consequence of the addition of a stable sea urchin cyclin to a cycling frog egg extract [11]. The echinoderm cyclin blocked exit from mitosis, causing a late anaphase arrest. In contrast, inhibition of APC arrested the extract in metaphase. Thus, the metaphase/anaphase transition required APC activity, but not inactivation of the sea urchin cyclin/Cdk. Similarly, in *Saccharomyces. cerevisiae*, mutations inactivating APC arrested cells prior to the separation of sister chromosomes, while expression of a stable Clb2, one of six B-type cyclins, arrested the cells after anaphase [12]. Work in budding yeast also identified a noncyclin target of APC action and a regulatory cascade connecting APC to the disjunction of sister chromosomes at metaphase/anaphase (for a review see [13]). Disjunction occurs upon the cleavage of proteins called cohesins, which hold the sister chromosomes together. This cleavage is promoted by separins, whose activation triggers the metaphase/anaphase transition. The activity of separins is inhibited by securins (encoded by *PDS1* in *S. cerevisiae*), which thereby prevent the progress to anaphase. Importantly, the securins are destroyed during mitosis in an APC-dependent process. While the evidence for these steps is excellent, the results do not preclude additional regulation of this cascade.

The suggestion that cyclin degradation is dispensable for chromosome disjunction could be extended to other mitotic events. Indeed, the failure of tested stable cyclins to block the progression of mitosis prior to late anaphase was taken as an indication that cyclin degradation did not regulate events before the final exit from mitosis [11,12]. However, there are many cyclins, three of which have mitotic roles in metazoans: cyclin A, cyclin B, and cyclin B3 [14]. Different cyclin/Cdk complexes have different specificities [14]; hence, it does not seem appropriate to consider their activities generically. Early experiments that tested the ability of a specific stable cyclin to arrest the metaphase/anaphase transition might have overlooked the capacity of other cyclins to influence this or other transitions.

Cyclins are degraded at different times during mitosis. As cyclin A degradation is known to precede cyclin B degradation in diverse species, there appears to be conservation in the order of destruction [15–19]. In *Drosophila*, cyclin A (CYC-A) is degraded prior to the metaphase/anaphase transition; the bulk of cyclin B (CYC-B), and virtually all spindle associated CYC-B, is degraded at the metaphase/anaphase transition; and cyclin B3 (CYC-B3) is degraded during anaphase [9,16,17,20–22]. This schedule of destruction of the different cyclins suggests that degradation of each cyclin might contribute to events at different times in mitosis. Indeed, expression of stable versions of each of the mitotic cyclins shows that they have distinct phenotypes that might represent arrest at successive stages of mitosis [9]. Demonstration of a clear temporal sequence in the onset of phenotypes of the different stable cyclins would provide support for the model that the schedule of cyclin degradation controls mitotic progression. Our analysis of mitotic progression in real-time shows that expression of each stable cyclin blocks only those mitotic events that occur after the cognate cyclin is ordinarily degraded. We have also confirmed the original suggestion that stable cyclin A (CYC-A^S) inhibits chromosome disjunction, and we provide evidence for a sequence of regulated mitotic events by defining

additional steps that require cyclin degradation. While CYC-A^S blocked the metaphase/anaphase transition, stable cyclin B (CYC-B^S) slowed anaphase A chromosome movements, blocked anaphase B spindle pole separation and cytokinesis, and promoted pole-to-pole oscillations of chromosomes. Stable cyclin B3 (CYC-B3^S) blocked cells in a late anaphase configuration except that deep cytokinetic furrows developed. These results offer strong support for the interpretation that cyclin destruction is not only essential for the return to interphase, but that destruction of individual cyclins controls and coordinates late mitotic events.

Results

Expression of stable mitotic cyclins results in distinct mitotic arrests

In an early attempt to investigate the role of mitotic cyclin degradation, we used transgenic flies carrying a heat shock-inducible sea urchin cyclin B that lacked the destruction box (Δ-90 cyclin B). This stable echinoderm cyclin blocks mitotic exit in vertebrates [11]; however, it was inactive in *Drosophila* (C.F.L., N.Y., and P.H.O., unpublished data) unless coexpressed with a vertebrate Cdk1 [9]. The sea urchin Δ-90 cyclin B interacted with the *Drosophila* and *Xenopus* Cdk1 kinases in vitro, but unlike the cognate cyclins, it failed to activate the *Drosophila* kinase and gave suboptimal activation of the *Xenopus* kinase (F.S. and P.H.O., unpublished data). These results suggested that the use of heterologous cyclins may not be reliable, and encouraged us to test each of the *Drosophila* mitotic cyclins.

We expressed stable versions of *Drosophila* cyclins, CYC-A^S, CYC-B^S (described in [23]), and CYC-B3^S (described in [9]), encoded by transgenes under the control of the heat-inducible promoter of the *Hsp70* gene. Following induced expression in the early embryo (G2 of cycle 14), cells arrested in mitosis with distinct phenotypes (Figure 1) similar to those described by Sigrist et al. [9]. These arrests are specific for the stable cyclins, as heat shock-induced expression of wild-type CYC-A or CYC-B does not perturb mitosis [24,25]. We examined these arrests using real-time analysis to determine whether these phenotypes are produced by the interruption of the normal sequence of mitotic events at different points, as predicted by a model in which the schedule of cyclin degradation guides progress of mitotic events.

CYC-A^S competes with endogenous CYC-A to provoke mitotic arrest

Drosophila embryos follow a precise mitotic program, and the knowledge of when cells go into mitosis and return to interphase allows us to assess the efficiency and duration of an induced mitotic arrest. A stable cyclin A construct was reported to give a delay at metaphase [9]. We have used a different stable cyclin A transgene and have examined somewhat different stages and conditions. Embryos with two copies of our CYC-A^S encoding transgene arrested more efficiently than embryos with one copy, arguing that the level of CYC-A^S is limiting. However, even with two copies, induction did not arrest cells until the following cell cycle. After expression in G2 of cell cycle 14 (embryos 165–195 min after egg deposition [AED]), embryos successfully, albeit slowly, transited mitosis 14 and arrested in mitosis 15 (Figure 2b; S.V. and P.H.O., unpublished data). Although stable cyclins are usually treated as dominant, CYC-A^S was more effective when endogenous CYC-A levels were reduced by mutation (S.V. and P.H.O., unpublished data; [9]). We conclude that competition with preexisting endogenous CYC-A limits the efficacy of newly induced CYC-A^S, and we suggest that second cycle arrest at mitosis occurs because the CYC-A^S gains a competitive advantage once the endogenous cyclins are degraded at the first mitosis.

Limited access to Cdk1, which appears to be fully bound by a cyclin in G2 of cycle 14 [26], might restrict activity of induced CYC-A^S. Though it had no effect on its own, coinduction of a *Drosophila Cdk1* transgene enhanced mitotic arrest by CYC-A^S. For example, Figure 2f

shows an embryo in which coinduction trapped all cells entering mitosis at metaphase, a result indicating more efficient arrest than previously reported [9]. Enhancement of the metaphase arrest by Cdk1 shows that action of CYC-A^S is, in part, limited by the availability of a kinase partner and argues that the arrest is mediated by a CYC-A/Cdk1 complex. Coinduction of CYC-A^S and Cdk1 gave a first cycle arrest when induced during cell cycle 16 when endogenous CYC-A levels are relatively low (Figure 2f) but still showed a second cycle arrest when induced in G2 of cycle 14 when CYC-A levels are high (Figure 2b). Taken together, our findings suggest that the arrest at metaphase by CYC-A^S is enhanced by conditions that increase its opportunity to compete with endogenous CYC-A.

CYC-A^S inhibits chromosome disjunction

We used a transgene consitutively expressing a histone-GFP fusion (H2AvD-GFP) to allow real-time visualization of chromosomes [27]. Embryos that were homozygous for CYC-A^S and *histone-GFP* transgenes were heat shocked in G2 of cycle 14, and real-time records were taken as cells entered mitosis 15. Events leading up to metaphase proceeded without noticeable deviation from wild-type, but in most cases, there was no indication of sister chromosome disjunction or anaphase chromosome movements. The arrest resembled a normal metaphase, and it was relatively static, with little change in the appearance of the chromosomes; we saw only slight "jiggling" of the chromosomes and of the position of the metaphase plate. The normal duration of metaphase 15 is about 2 min. In contrast, individual cells arrested with CYC-A^S were followed for up to 25 min, with no release of the arrest seen in the majority of cases (see Movie 1in supplementary material). We conclude that CYC-A^S can prevent progress to anaphase.

While the majority of our records showed a static metaphase, some cells (on the order of 10%) expressing CYC-A^S had a prolonged metaphase followed by anaphase (Movie 2). In contrast to the static block, which provided little detail regarding the step inhibited by CYC-A^S, the prolonged mitoses revealed that chromosome disjunction itself is inhibited. We followed six cells that were in metaphase at the start of the record and remained arrested for at least 7.5 min before escaping. Chromosome disjunction, which appears instantaneous in wild-type (all the kinetochores appear to separate together, and chromosomes arms pull apart over 20–45 s), was greatly prolonged by the presence of CYC-A^S, and anaphase progression was disturbed. Chromosome disjunction in cell 1 (see Movie 2 in supplementary material) was drawn out over 2.5 min. It began with subtle irregularities in the metaphase plate that grew as pieces of chromatin pulled away, eventually resolving into two chromosomal masses with bridging that disappeared as the masses moved apart. These masses separated fully at about half the normal anaphase rate and then decondensed. While movements out of the focal plane truncated some records, disjunction was prolonged in all six cells. When observed, the anaphase movements were slowed, and in cells 2 and 3, anaphase separation was incomplete (Figure 3b; see Movie 2 in supplementary material). The slowing of anaphase could be secondary to the inhibition of disjunction or it could be an independent effect of CYC-A^S. We conclude that CYC-A^S inhibits sister chromosome disjunction. It should be noted that cells escaping the metaphase arrest also exited mitosis without showing evidence of a later arrest point.

The endogenous mitotic cyclins are still degraded during a CYC-A^S arrest [9], suggesting that the activity of the CYC-A^S/Cdk1 complex may be sufficient to maintain the metaphase block. In a preliminary test of this hypothesis, we treated arrested embryos with the general kinase inhibitor 6-dimethylaminopurine (6-DMAP [28]. Embryos fixed 1 min following the addition of 6-DMAP exhibited reduction in phospho-histone staining (a marker for mitosis), numerous highly defective anaphases, as well as decondensing DNA masses (Figures 3c,d). The defective anaphases featured extensively connected DNA masses, suggesting incomplete chromosome disjunction. Numerous factors, such as the abruptness of the kinase inactivation or the lack of

specificity of 6-DMAP, might contribute to the highly abnormal mitotic exit. Nonetheless, the rapid reversal of mitotic features implies that kinase activity is required to maintain numerous features of the metaphase arrest.

Chromosomes oscillate from pole to pole in the CYC-B^S arrest

Expression of our stable cyclin B transgene often arrested cells at the first mitosis after induction (Figure 2c), suggesting that action of CYC-B^S is not limited in the same way or to the same degree as CYC-A^S. Nonetheless, the efficiency of the arrest improved with the transgene dose and with Cdk1 coexpression (Figure 2c). At the terminal arrest, chromosomes were disjoined and chaotically arranged around the midpoint of the spindle (Figures 1b and 2c, inset; [6, 9]). We examined the approach to this arrest in real-time to determine the point of deviation from normal mitotic progression.

Embryos that were homozygous for stable cyclin B and *histone-GFP* transgenes were heat shocked and observed. We observed no significant differences in progression through prophase and metaphase as compared to wild-type (see Movie 3 in supplementary material). Sister chromosomes appeared to disjoin and move toward opposite poles normally, albeit slowly (see below) (Figure 4a; Movie 3 in supplementary material). As the trailing tips of the longer chromosomes lost contact with their sisters, anaphase movement stopped and, after a pause, chromosomes moved slowly along chaotic paths back to the midpoint of the spindle (Figure 4; Movie 3 in supplementary material). The chromosomes, though clustered near the middle of the spindle, took erratic and independent excursions toward the poles (see Movie 4 in supplementary material). The rate of this poleward movement, roughly 6 μm/min, varied from chromosome to chromosome but approximated anaphase rates (see below). Excursions, which were led by the kinetochore, stopped abruptly before the chromosome reached the pole (Figure 4b; see Movies 3–5 in supplementary material). After an excursion, the chromosome slowly drifted back to the middle of the spindle in a movement that was not led by the kinetochore (Figure 4b; see Movie 4 in supplementary material). Sometimes this gradual movement was interrupted by a sudden acceleration toward the opposite pole in a movement that was led by the kinetochore and typically carried the chromosome across the middle of the spindle and close to the other pole (see Movie 5 in supplementary material). We conclude that CYC-B^S provokes chromosome movements unlike those of anaphase, and we suggest that CYC-B degradation is required for kinetochore-spindle interactions appropriate to anaphase. Importantly, though the final arrest does not represent a simple block of anaphase movements, the progress of mitosis in the presence of CYC-B^S deviates from normal only after metaphase/anaphase, the stage at which the bulk of the endogenous CYC-B is degraded [16, 22].

CYC-B^S affects progression of anaphase events

To identify specific mitotic events disrupted by CYC-B^S, we measured the rate and extent of chromosome separation in control and CYC-B^S-expressing cells. Separation was followed until chromosomes decondensed (control) or until poleward chromosome movements faltered (CYC-B^S-expressing cells). Expression of CYC-B^S retarded chromosome separation within about 20 s of metaphase/anaphase, slowed chromosome movement more than 2-fold (2.2 ± 0.3 μm/min versus a control rate of 5.9 ± 0.8 μm/min) (Figures 4 and 5a), and reduced the final extent of separation (~7 μm) to just over half of control separation (~12 μm) (Figure 5a).

Anaphase chromosome movement has two stages: sister chromatids disjoin and move poleward during anaphase A, then the spindle poles move apart, further separating the chromosomes during anaphase B. We asked if the diminished extent of chromosome separation in cells expressing CYC-B^S corresponded to a failure of pole separation/spindle elongation. The centrosomes that mark the spindle poles were detected by immunostaining for γ-tubulin, and the distance between poles was measured. In control cells, spindle length at metaphase (7.1 ±

1μm) began to increase at the midpoint of chromosome separation and almost doubled by the end of anaphase (12.8 ± 1μm) (Figure 5b; data not shown). In cells arrested with CYC-B^S, spindle length (6.9 ± 1μm) was the same as in control metaphase cells (Figure 5b). We conclude that persistent CYC-B slows anaphase A and blocks anaphase B.

CYC-B3^S blocks mitosis after anaphase B spindle pole separation

Since CYC-B3 is degraded only after metaphase/anaphase [21], the early events of mitosis should not be impeded by CYC-B3^S. We examined fixed and live embryos to determine which mitotic events were blocked. Induction of CYC-B3^S in embryos that were homozygous for the transgene caused arrest in the first mitosis (Figure 2d). Real-time analysis revealed that cells expressing CYC-B3^S proceeded through the metaphase/anaphase transition with normal timing and separated their chromosomes with kinetics similar to wild-type but then arrested with condensed chromosomes at the poles (Figure 5a; see Movies 6–8 in supplementary material). Continuous observation showed that arrest with the chromosomes congregated at the poles was stable for at least 20 min in most cases. Unlike the results with CYC-B^S, spindle length at the CYC-B3^S arrest matched the length of spindles in control cells at the end of mitosis, indicating that anaphase B was not blocked (Figure 5b). However, unlike control cells, in which the spindle matures after anaphase to produce a stereotyped bundle of compacted tubules comprising the midbody (Figure 6e), the spindles of CYC-B3^S-expressing cells lacked compacted foci of tubulin staining or showed foci lacking the symmetry and organization of the normal midbody (Figures 1c and 6c; data not shown). We conclude that cells expressing CYC-B3^S deviate from normal mitotic progression only after anaphase B, and late events in spindle reorganization and exit from mitosis are blocked.

In addition to the stable arrest with chromosomes at the poles, a few cells (on the order of 10%) exhibited a more dynamic arrest in which individual chromosomes left the spindle pole and traveled back along the spindle at rates comparable to anaphase rates. Occasionally, these chromosomes reached the opposite pole. Often, in cells where this phenomenon occurs, the spindle rotated in the plane of the epithelium (examples can be seen indicated by arrows in Movie 6 in supplementary material). Sigrist et al. also observed a minor class of arrested cells having some chromosomes away from the poles [9]. While the correspondence is uncertain, our real-time observations are consistent with the rare class of cells described in fixed embryos.

Cytokinetic furrow formation can proceed in cells expressing CYC-B3^S

Background fluorescence from the histone-GFP sometimes allowed us to see cell outlines in real-time. In such cases, cells expressing CYC-B3^S were observed to develop an invagination at the time expected for cytokinetic furrow formation (Figure 6a; see Movies 7 and 8 in supplementary material). Since furrow formation normally initiates toward the end of anaphase, its timing could be influenced by the sequential destruction of cyclins. To explore this, we looked for furrow formation at the arrests induced by each of the stable cyclins. To better visualize furrow formation, we stained fixed embryos with the F-actin stain, phalloidin, which stains the cell cortex and cleavage furrows. While the other arrests showed an undisturbed cell perimeter (data not shown), cells arrested by expression of CYC-B3^S included many examples in which deep furrows were evident (Figure 6c). The furrows often appeared to bisect the persisting spindle without obvious pinching of the spindle fibers in the middle. The furrows were also marked by anillin staining, an actin binding protein that localizes to the furrow [29], as in normal cytokinesis (Figure 6d). The cytokinetic furrow usually does not invaginate deeply until telophase. We conclude that CYC-B^S can block cytokinetic furrow formation, while CYC-B3^S cannot, and we suggest that, once initiated, cytokinesis continues to progress, while CYC-B3^S blocks other aspects of mitotic exit, such as chromosome decondensation, nuclear envelope reformation, and spindle reorganization.

Discussion

The complex steps executing chromosome separation and exit from mitosis could potentially unfold as an unimpeded sequence, like toppling dominoes. However, our results identify a novel coupling of mitotic exit events to the regulatory machinery of the cell via a dependency on cyclin degradation. CYC-B^S blocked anaphase B and cytokinesis and led to dynamic oscillations of the disjoined chromosomes (Figures 4 and 5; see Movies 3–5 in supplementary materials). While lacking these activities, CYC-B3^S inhibited final spindle reorganization and exit from mitosis (Figure 6; see Movies 6–8 in supplementary material). We also provide strong support for the previous suggestion that CYC-A, and not the other mitotic cyclins, inhibits chromosome disjunction (Figure 3; see Movies 1 and 2 in supplementary material). The differing actions of the cyclins match the normal sequence of degradation of mitotic cyclins, with each cyclin being degraded in advance of the events that it inhibits. Not all mitotic events are arrested in concert; for example, arrest of chromosome decondensation by CYC-B3^S does not block the progression of cytokinesis (Figure 6; see Movies 7 and 8 in supplementary material). This miscoordination suggests that the interdependencies of steps in mitosis are not sufficient to direct the orderly sequence of mitotic events, at least in the face of perturbation. Together, our findings suggest that the schedule of destruction of different cyclins contributes to the timing and coordination of mitotic events (Figure 7).

Control of chromosome disjunction by CYC-A

The observation that CYC-A^S arrested cells in metaphase suggests that, normally, CYC-A must be degraded in order to disjoin sister chromosomes. Consistent with this interpretation, recent reports have implicated cyclin degradation in the regulation of the metaphase/anaphase transition. Irradiation of *Drosophila* embryos induces a prolonged metaphase, during which damage appears to be repaired [30]. CYC-A was implicated in this arrest by the finding that mutant embryos with reduced CYC-A levels fail to arrest at metaphase. Similarly, the ability of DNA damage to induce an arrest prior to DNA segregation in *S. cerevisiae* requires the presence of either Clb5 or Clb6 [31]. While homology is not sufficient to define a homolog of metazoan cyclin A among *S. cerevisiae* cyclins, common functional attributes suggest that Clb5/6 and cyclin A are analogs [14,31,32]. We propose that A-like cyclins in diverse species act to inhibit the metaphase/anaphase transition and that progress to later steps requires degradation of these cyclins.

The degree to which CYC-A^S prolonged mitosis depended on the experimental conditions. The differences appear to be attributable to a limited ability of CYC-A^S to compete with preexisting endogenous CYC-A (see Results). Delayed metaphase/anaphase transitions were gradual, with disjunction drawn out over a few minutes, and sometimes ineffective (Figure 4; see Movie 2 in supplementary material). Ordinarily, the disjunction of chromosomes is abrupt and synchronous, occurring within several seconds in *Drosophila*. The abruptness of the transition suggests that a switch-like regulatory circuit must govern its execution. The finding that CYC-A^S can prolong disjunction suggests that CYC-A inhibits events that are downstream of the switch or part of the switch that usually imparts all-or-nothing behavior.

The abrupt activation of chromosome disjunction is likely to involve multiple regulatory inputs. Indeed, identification of *Drosophila* analogs of the securins, separins, and cohesins suggests that *Drosophila* uses a conserved pathway to regulate chromosome disjunction [33–35]. Consistent with this, stabilization of Pimples (PIM), the securin, shows that degradation of this protein promotes disjunction of sister chromosomes [35]. How might cyclin degradation interface with securin degradation to activate sister chromosome disjunction? CYC-A appears to block chromosome disjunction independently of securin, because persistence of CYC-A^S does not block PIM degradation (O. Leismann and C.F. Lehner, personal communication). While there is not enough data in either *S. cerevisiae* or *Drosophila* to define the regulatory

relationship, we suggest the model described in Figure 7a as a simple proposal to account for data from both systems. This proposal suggests that separins are inhibited incompletely by securin or CYC-A/Cdk1 alone, but effectively by the combination.

The timing of CYC-A destruction suggests that it precedes PIM destruction in a pathway leading to chromosome disjunction. CYC-A immunofluorescence shows both stained and unstained metaphases, and the proportion of unstained metaphases (about 30%) suggests that CYC-A is degraded about 15–35 s prior to chromosome disjunction [30]. During this interval, we expect that a target of CYC-A/Cdk1 kinase activity is dephosphorylated, separins are activated, and cohesins are cleaved. It seems likely that numerous regulatory interactions might operate to make cohesin cleavage fast and the metaphase/anaphase transition abrupt. The degradation of PIM, which takes place around the time of the metaphase/anaphase transition [35,36], might be one of the changes promoting rapid activation of the separins.

Unlike the arrests induced by the other stable cyclins, the metaphase arrest induced by CYC-A^S appears to be a normal mitotic configuration. We interpret this to mean that CYC-A can arrest progression of all mitotic events in a concerted fashion. The ability to impose a concerted arrest is consistent with a role in checkpoint arrest of the cycle; however, reversal of such a block would have to be abrupt to avoid the defects we see associated with prolongation of chromosome disjunction (Figure 3b; see Movie 2 in supplementary material).

CYC-B^S derails mitosis in mid-anaphase

CYC-B antibody stains all metaphase cells but fails to stain cells that have clearly progressed to anaphase, arguing that CYC-B is normally degraded rapidly at the metaphase/anaphase transition [16]. Consistent with this, spindle-associated fluorescence from a CYC-B-GFP fusion protein disappeared before anaphase, although a weaker cytoplasmic fluorescence persisted [22]. Onset of CYC-B degradation at metaphase/anaphase implies that CYC-B^S should have its earliest impact after metaphase. Fitting this prediction, CYC-B^S was previously reported to arrest mitosis with disjoined, but not separated, chromosomes (Figure 1; [37]). However, this seemed unlikely to be a simple arrest configuration. Since a balance of tension is thought to retain chromosomes at the metaphase plate, disjunction ought to free the sister chromosomes to move to the poles [13]. Indeed, real-time results revealed that early mitotic events were normal and that anaphase movements followed chromosome disjunction. The unusual terminal configuration followed specific disruptions in anaphase.

The earliest defect following expression of CYC-B^S was the slowing of anaphase A chromosome movements (Figure 4 and 5a; see Movies 3 and 4 in supplementary material). Coordinated action of motor proteins at the kinetochore and spindle microtubule depolymerization usually drive these movements [38]. Our data do not identify the aspect of movement that is inhibited, but they show that timely degradation of CYC-B is essential for normal chromosome movement.

CYC-B persistence also blocks anaphase B pole separation (Figure 5b). Spindle elaboration relies on a balance of forces from numerous motor proteins. Recent work suggests that the balance of forces tips toward pole separation upon downregulation of the minus end-directed motor Ncd [39]. Accordingly, our observations could be explained if CYC-B degradation triggered downregulation of Ncd and so induced pole movements. Regardless of the mechanism, our findings show that anaphase B initiation is regulated and that it could be timed by the schedule of CYC-B degradation.

Mitosis does not simply arrest at the point of its inhibition by CYC-B^S. After the slowed anaphase movements, the chromosomes pause, then move discoordinately back to the midpoint of the spindle (Figure 4, see Movies 3–5 in supplementary material). From there, the

chromosomes take frequent excursions toward the poles, often oscillating back and forth between one pole and the other. These oscillations resemble those of the unpaired sex chromosome in male meiosis in grasshoppers [40]. Without a balancing pull toward the opposite pole, chromosomes move toward the pole to which they are attached. But why do they oscillate? According to one interpretation, instability in kinetochore-spindle interactions leads to a cycle of detachment and eventual reattachment to spindle fibers from the opposite pole and subsequent movement to that pole. Physical pulling indicated that chromosomes were not always attached to the spindle but also demonstrated that tension stabilizes attachment. It was inferred that these features cooperate to promote the attachment of the two kinetochores of normal chromosomes to opposite poles during prometaphase, as this ought to be the only stable outcome (for a review see [41]). Because of its contribution to the alignment of chromosomes, tension-dependent kinetochore-spindle attachment is thought to be an essential feature of prometaphase.

The stability of kinetochore-spindle attachment becomes independent of tension by the time of anaphase. This is necessary because tension is lost when chromosomes become univalent upon disjunction, yet chromosomes must retain their orientation to a single pole for orderly distribution to daughter nuclei. It is not known what controls the change in stability of kinetochore-spindle attachment between prometaphase and anaphase. Our finding that persistence of CYC-B results in continued unstable attachment suggests that degradation of CYC-B is required for this transition in stability. In contrast to the unstable kinetochore-spindle interaction at the CYC-B^S arrest, chromosomes are held at the poles for as long as 20 min at the CYC-$B3^S$ arrest. We propose that the unstable kinetochore-spindle attachment that prevails in prometaphase can be countered by tension during prometaphase/metaphase or by degradation of CYC-B at the metaphase/anaphase transition. Additionally, we suggest that the period between the degradation of CYC-B and destruction of CYC-B3 provides a mitotic phase of stable kinetochore-spindle attachment during which chromosomes can be faithfully segregated. To probe the mechanism of this effect, it will be interesting to examine the influence of CYC-B/Cdk1 on putative regulators of chromosome congression such as CENP-E [17].

Our CYC-B^S results differ from some related analyses in other systems. Stabilization of the *S. cerevisiae* Clb2 arrested cells with an elongated spindle [12], which suggests the completion of anaphase. However, differences in the biology and uncertain analogies among cyclins make comparisons to yeast difficult. Introduction of a stable sea urchin Δ-90 cyclin B into *Xenopus* extract systems [11] and into mammalian tissue culture cells [42] allowed chromosome separation to the poles. However, when tested in sea urchin, this echinoderm Δ-90 cyclin B induced a phenotype consistent with the one we have described [8]. Furthermore, a stable version of vertebrate cyclin B2, one of the two closely related B type cyclins in vertebrates, blocked HeLa cells with a metaphase-like arrest with chromosomes "not properly aligned at the metaphase plate" [7], which is consistent with the arrest we have characterized. Based on observations that heterologous cyclin and Cdk combinations, particularly the echinoderm cyclin B with *Drosophila* Cdk, have limited activity (see Results), we suggest that discordant observations result from the use of heterologous cyclins and that the results we report will extend to other metazoan systems.

CYC-B3 blocks the final events of mitosis without blocking cytokinesis

Following the expression of CYC-$B3^S$, prophase, meta-phase, and anaphase A and B all occur with the normal timing and kinetics (Figure 6; see Movie 6 in supplementary materail). Once anaphase is complete, however, CYC-$B3^S$ blocks further nuclear and spindle events: chromosomes remain condensed, the nuclear membrane fails to reform, and the spindle remains intact without maturing to its late mitotic configuration with a prominent midbody (Figure 5; see Movies 6–8 in supplementary material). In many arrested cells, cytokinesis proceeds,

bifurcating the spindle and separating the two polar clusters of chromosomes. Furrowing was detected as chromosomes reached the poles, and both live and fixed data suggest that furrows are deep, stable, and perhaps complete. Double labeling reveals cells that stain for CYC-B3, but not CYC-B, indicating that CYC-B3 is normally degraded after CYC-B and hence after the metaphase/anaphase transition [9]. In addition, CYC-B3 labeling has disappeared by the time anaphase separation of chromosomes is complete [21]. Our results show that mitosis progresses normally to late anaphase in the presence of CYC-B3^{S}, and only at this point do we see an arrest of multiple late mitotic events.

Cytokinetic furrow formation in cells with condensed chromosomes implies that cytokinesis is not coupled to the progress of nuclear or cytoplasmic events by direct dependencies. Instead, the results suggest that the onset of cytokinesis is regulated by the schedule of cyclin destruction. Perhaps the different abilities of CYC-B and CYC-B3 to inhibit furrow formation allow a window of opportunity for timely initiation of furrow formation. This window would be created by degradation of CYC-B before CYC-B3 but might be offset from the time of degradation by a lag time required for the dephosphorylation of relevant targets. Consistent with this idea, furrow formation commences earlier than normal in embryos deficient in CYC-B [25].

Cytokinesis without mitotic progression produced a furrow that appears to cut through the spindle that lacks the compact microtubular midbody structure. Thus, in the context of the CYC-B3^{S} arrest, furrow formation can occur in the absence of a spindle midbody, a structure that has been proposed to be essential for cytokinesis [43]. Nonetheless, the gene products normally recruited to the midbody may be recruited to the midzone in the absence of morphological specialization and thereby play their proposed roles in the stabilization of the cytokinetic furrow [44,45].

The schedule of cyclin degradation results in sequential release of constraints

The three stable cyclins differ in their abilities to block specific mitotic events, each blocking events occurring at the time of degradation of the endogenous cognate cyclin. As the action of stable cyclins, in those cases in which it has been tested, is enhanced by coexpression of the kinase partner Cdk1, we believe that these blocks are mediated by the corresponding cyclin/Cdk1 complexes. We propose that the specificity results because the different cyclin/Cdk1 complexes differ in their ability to target particular cellular substrates, as suggested by numerous biochemical investigations (for a review see [14]). During the exit from mitosis, differences in cyclin/Cdk1 specificity, in conjunction with the ordered degradation of the different cyclins, may be an important way of coupling the mechanics of cell division to the regulatory machinery. By degrading each cyclin in turn, the inhibitions established at each transition point are relieved and the cellular processes of chromosome disjunction, anaphase movements, and cytokinesis can proceed with the proper kinetics (Figure 7b).

Materials and methods

Control embryos are of the strain Sevelen. The transgenes used here have been described previously; hsp70-*cyc-A*^{S} (Δ-169) and hsp70-*cyc-B*^{S} (Δ-46) [23], hsp-70-*cyc-B3*^{S} (Δ-91) [9], hsp-*cdk-1* [46], and histone 2AvD-GFP (histone-GFP) [27]. All transgenes are homozygous viable. We performed crosses with the histone-GFP line to isolate a chromosome with a single P element insertion containing the transgene. Standard crossing schemes were used to generate homozygous lines carrying an inducible cyclin transgene together with histone 2AvD-GFP, or with hsp-Cdk1.

Embryos were collected on grape juice agar plates for 30 min and aged for 150–165 min at 25°C. Embryos were heat shocked by floating grape juice agar plates on a covered 37°C water

bath for 30 min. Under these conditions, control heat shocks of Sevelen embryos showed no disruption in mitotic domain patterns, and control heat shocks of histone-GFP embryos, when examined in real-time, showed no effect on mitotic progression. Embryos were then aged at 25°C for at least 30 min before real-time analysis (see below) or aged at 25°C for 60–75 min before formaldehyde fixation. Embryos to be fixed were washed into a basket, dechorionated with 50% bleach, washed with water, then fixed in a 1:1 mixture of heptane and 37% formaldehyde for 5 min (or 3.7% formaldehyde for 20 min for γ-tubulin staining). Embryos were then devitellinized with methanol, or by hand for subsequent phalloidin staining, and washed in phosphate-buffered saline containing 0.1% Triton X-100 (PTX).

For the 6-DMAP experiment, embryos that were homozygous for hsp70-*cyc-A* and hsp-*cdk-1* were heat shocked, aged, and dechorionated as described above. Embryos were then treated with octane for 4 min in order to permeabilize the vitelline membrane and transferred to Schneider's medium containing 10 mM 6-DMAP (no 6-DMAP for control) for 1 min. Embryos were then fixed with 37% formaldehyde and stained as described.

Our standard protocol for antibody staining was to block embryos for 1 hr at room temperature (RT) in PTX + 5% normal donkey serum (NDS). Primary antibody incubations took place in PTX + 5% NDS for 4 hr at RT or overnight at 4ΔC. Embryos were washed between primary and secondary antibodies with PTX + 5% NDS for 3 × 10 min at RT. Fluorescent-labeled secondary antibody or phalloidin incubations took place in PTX + 5% NDS for 1 hr at RT. Embryos were then washed with PTX for 3 × 10 min, with a 4 min Hoechst 33,258 (1μg/ml in PTX) staining step between the first and second washes. Embryos were mounted on microscope slides using Fluoromount-G. Primary antibodies used in this study include α-tubulin (Sigma; 1:150), phospho-histone H3 (Upstate Biotechnology; 1:1000), γ-tubulin (Sigma; 1:100), and anillin (provided by Christine Field; 1:1000). Fluorescently labeled phalloidin was from Molecular Probes (Fluorescein, Texas Red). Goat anti-rabbit and goat anti-mouse fluorescently labeled secondaries were from Jackson Laboratories.

Embryos used for real-time analysis were aged and heat shocked as described, then dechorionated with 50% bleach, rinsed with water, and mounted under halocarbon oil on a custom made slide (Omax). All real-time records were taken from embryos expressing the *histone-GFP* transgene to mark the chromosomes. Images were captured with a Princeton Instruments CCD on an Olympus inverted microscope using the time lapse feature of the DeltaVision microscopy system software. The final QuickTime movies were produced using Adobe Premiere software.

For the measurements of anaphase chromosome separation, the distance between the leading edge of separating chromosome masses was calculated for each frame using the distance measuring function of the DeltaVision microscopy system software. The zero time point was defined as the frame preceding the first indication of chromosome separation. In order to calculate the rates of early anaphase chromosome movements for wild-type and CYC-B^S, the slope of the best fit line between the 18 s and 42 s time points was calculated for each individual record. The individual slopes were then averaged, and the standard deviation calculated. For measuring spindle length, fixed cells were stained for γ-tubulin, which marks the centrosomes, and the distance between γ-tubulin spots was measured using the distance measuring function of the DeltaVision microscopy system software.

Supplementary Material

Refer to Web version on PubMed Central for supplementary material.

Acknowledgments

We thank Christian Lehner for providing us with the hsp-70-*cyc-B3*^{S} (Δ-91) fly line, Robert Saint for the histone 2AvD-GFP fly line, and Christine Field for anillin antibody. We are grateful to Smruti Vidwans, Paul DiGregorio, Simon Prochnik, Renny Feldman, Arnaud Echard, and other O'Farrell lab members for helpful discussions and critical reading of the manuscript and to Tony Shermoen for invaluable technical assistance. D.H.P. is supported by the Dr. and Mrs. Bernard Kramer Scholarship from the ARCS Foundation and by National Institutes of Health training grant #T32HD07470. This work was funded by National Institutes of Health grant #GM37193 to P.H.O.

References

1. Murray, AW.; Hunt, T. The Cell Cycle. New York: Oxford University Press; 1993.
2. Zachariae W, Nasmyth K. Whose end is destruction: cell division and the anaphase-promoting complex. Genes Dev 1999;13:2039–2058. [PubMed: 10465783]
3. Murray AW, Solomon MJ, Kirschner MW. The role of cyclin synthesis and degradation in the control of maturation promoting factor activity. Nature 1989;339:280–286. [PubMed: 2566918]
4. Luca FC, Shibuya EK, Dohrmann CE, Ruderman JV. Both cyclin A delta 60 and B delta 97 are stable and arrest cells in M-phase, but only cyclin B delta 97 turns on cyclin destruction. EMBO J 1991;10:4311–4320. [PubMed: 1836759]
5. Ghiara JB, Richardson HE, Sigimoto K, Henze M, Lew DJ, Wittenberg C, et al. A cyclin B homolog in *S. cerevisiae*: chronic activation of the Cdc28 protein kinase by cyclin prevents exit from mitosis. Cell 1991;65:163–174. [PubMed: 1849458]
6. Su TT, Sprenger F, DiGregorio PJ, Campbell SD, O'Farrell PH. Exit from mitosis in *Drosophila* syncytial embryos requires proteolysis and cyclin degradation, and is associated with localized dephosphorylation. Genes Dev 1998;12:1495–1503. [PubMed: 9585509]
7. Gallant P, Nigg EA. Cyclin B2 undergoes cell cycle-dependent nuclear translocation and, when expressed as a nondestructible mutant, causes mitotic arrest in HeLa cells. J Cell Biol 1992;117:213–224. [PubMed: 1532584]
8. Hinchcliffe EH, Cassels GO, Rieder CL, Sluder G. The coordination of centrosome reproduction with nuclear events of the cell cycle in the sea urchin zygote. J Cell Biol 1998;40:17–26.
9. Sigrist S, Jacobs H, Stratmann R, Lehner CF. Exit from mitosis is regulated by *Drosophila* fizzy and the sequential destruction of cyclins A, B and B3. EMBO J 1995;14:4827–4838. [PubMed: 7588612]
10. Rimmington G, Dalby B, Glover DM. Expression of N-terminally truncated cyclin B in the *Drosophila* larval brain leads to mitotic delay at late anaphase. J Cell Sci 1994;107:2729–2738. [PubMed: 7876341]
11. Holloway SL, Glotzer M, King RW, Murray AW. Anaphase is initiated by proteolysis rather than by the inactivation of maturation-promoting factor. Cell 1993;73:1393–1402. [PubMed: 8391932]
12. Surana U, Amon A, Dowzer C, McGrew J, Byers B, Nasmyth K. Destruction of the CDC28/CLB mitotic kinase is not required for the metaphase to anaphase transition in budding yeast. EMBO J 1993;12:1969–1978. [PubMed: 8491189]
13. Nasmyth K, Peters JM, Uhlmann F. Splitting the chromosome: cutting the ties that bind sister chromatids. Science 2000;288:1379–1385. [PubMed: 10827941]
14. Roberts JM. Evolving ideas about cyclins. Cell 1999;98:129–132. [PubMed: 10428024]
15. Pines J, Hunter T. Human cyclin A is adenovirus E1A-associated protein p60 and behaves differently from cyclin B. Nature 1990;346:760–763. [PubMed: 2143810]
16. Lehner CF, O'Farrell PH. The roles of Drosophila cyclins A and B in mitotic control. Cell 1990;61:535–547. [PubMed: 2139805]
17. Whitfield WG, Gonzalez C, Maldonado-Codina G, Glover DM. The A- and B-type cyclins of *Drosophila* are accumulated and destroyed in temporally distinct events that define separable phases of the G2-M transition. EMBO J 1990;9:2563–2572. [PubMed: 2142452]
18. Minshull J, Golsteyn R, Hill CS, Hunt T. The A- and B-type cyclin associated cdc2 kinases in *Xenopus* turn on and off at different times in the cell cycle. EMBO J 1990;9:2865–2875. [PubMed: 2143983]
19. Luca FC, Ruderman JV. Control of programmed cyclin destruction in a cell-free system. J Cell Biol 1989;109:1895–1909. [PubMed: 2530237]

20. Maldonado-Codina G, Glover DM. Cyclins A and B associate with chromatin and the polar regions of spindles, respectively, and do not undergo complete degradation at anaphase in syncytial *Drosophila* embryos. J Cell Biol 1992;116:967–976. [PubMed: 1531147]
21. Jacobs HW, Knoblich JA, Lehner CF. *Drosophila* cyclin B3 is required for female fertility and is dispensable for mitosis like cyclin B. Genes Dev 1998;12:3741–3751. [PubMed: 9851980]
22. Huang J, Raff JW. The disappearance of cyclin B at the end of mitosis is regulated spatially in *Drosophila* cells. EMBO J 1999;18:2184–2195. [PubMed: 10205172]
23. Sprenger F, Yakubovich N, O'Farrell PH. S-phase function of *Drosophila* cyclin A and its downregulation in G1 phase. Curr Biol 1997;7:488–499. [PubMed: 9210381]
24. Lehner CF, Yakubovich N, O'Farrell PH. Exploring the role of *Drosophila* cyclin A in the regulation of S phase. Cold Spring Harb Symp Quant Biol 1991;56:465–475. [PubMed: 1840259]
25. Knoblich JA, Lehner CF. Synergistic action of *Drosophila* cyclins A and B during the G2-M transition. EMBO J 1993;12:65–74. [PubMed: 8428595]
26. Edgar BA, Sprenger F, Duronio RJ, Leopold P, O'Farrell PH. Distinct molecular mechanism regulates cell cycle timing at successive stages of *Drosophila* embryogenesis. Genes Dev 1994;8:440–452. [PubMed: 7510257]
27. Clarkson M, Saint R. A His2AvDGFP fusion gene complements a lethal His2AvD mutant allele and provides an in vivo marker for *Drosophila* chromosome behavior. DNA Cell Biol 1999;18:457–462. [PubMed: 10390154]
28. Vesely J, Havlicek L, Strnad M, Blow JJ, Donella-Deana A, Pinna L, et al. Inhibition of cyclin-dependent kinases by purine analogues. Eur J Biochem 1994;224:771–786. [PubMed: 7925396]
29. Field CM, Alberts BM. Anillin, a contractile ring protein that cycles from the nucleus to the cell cortex. J Cell Biol 1995;131:165–178. [PubMed: 7559773]
30. Su TT, Jaklevic B. DNA damage leads to a cyclin A-dependent delay in metaphase-anaphase transition in the *Drosophila* gastrula. Curr Biol 2001;11:8–17. [PubMed: 11166174]
31. Meyn MA III, Holloway SL. S-phase cyclins are required for a stable arrest at metaphase. Curr Biol 2000;10:1599–1602. [PubMed: 11137013]
32. Cross FR, Jacobson MD. Conservation and function of a potential substrate-binding domain in the yeast Clb5 B-type cyclin. Mol Cell Biol 2000;20:4782–4790. [PubMed: 10848604]
33. Warren WD, Steffensen S, Lin E, Coelho P, Loupart M, Cobbe N, et al. The *Drosophila* RAD21 cohesin persists at the centromere region in mitosis. Curr Biol 2000;10:1463–1466. [PubMed: 11102811]
34. Warren WD, Lin E, Nheu TV, Hime GR, McKay MJ. Drad21, a *Drosophila* rad21 homologue expressed in S-phase cells. Gene 2000;250:77–84. [PubMed: 10854781]
35. Leismann O, Herzig A, Heidmann S, Lehner CF. Degradation of *Drosophila* PIM regulates sister chromatid separation during mitosis. Genes Dev 2000;14:2192–2205. [PubMed: 10970883]
36. Stratmann R, Lehner CF. Separation of sister chromatids in mitosis requires the *Drosophila* pimples product, a protein degraded after the metaphase/anaphase transition. Cell 1996;84:25–35. [PubMed: 8548823]
37. Sigrist SJ, Lehner CF. *Drosophila* fizzy-related down-regulates mitotic cyclins and is required for cell proliferation arrest and entry into endocycles. Cell 1997;90:671–681. [PubMed: 9288747]
38. Heald R. Motor function in the mitotic spindle. Cell 2000;102:399–402. [PubMed: 10966101]
39. Sharp DJ, Brown HM, Kwon M, Roger GC, Holland G, Scholey JM. Functional coordination of three mitotic motors in *Drosophila* embryos. Mol Biol Cell 2000;11:241–253. [PubMed: 10637305]
40. Nicklas RB. Recurrent pole-to-pole movements of the sex chromosome during prometaphase I in Melanoplus differentialis spermatocytes. Chromosoma 1961;12:97–115. [PubMed: 13728791]
41. Nicklas RB. How cells get the right chromosomes. Science 1997;275:632–637. [PubMed: 9005842]
42. Wheatley SP, Hinchclife EH, Glotzer M, Hyman AA, Sluder G, Wang YI. CDK1 inactivation regulates anaphase spindle dynamics and cytokinesis in vivo. J Cell Biol 1997;138:385–393. [PubMed: 9230080]
43. Gatti M, Giansanti MG, Bonaccorsi S. Relationships between the central spindle and the contractile ring during cytokinesis in animal cells. Microsc Res Tech 2000;49:202–208. [PubMed: 10816260]

44. Severson AF, Hamill DR, Carte JC, Schumacher J, Bowerman B. The aurora-related kinase AIR-2 recruits ZEN-4/CeMKLP1 to the mitotic spindle at metaphase and is required for cytokinesis. Curr Biol 2000;10:1162–1171. [PubMed: 11050384]

45. Kaitna S, Mendoza M, Jantsch-Plunger V, Glotzer M. Incenp and an aurora-like kinase form a complex essential for chromosome segregation and efficient completion of cytokinesis. Curr Biol 2000;10:1172–1181. [PubMed: 11050385]

46. Stern B, Ried G, Clegg NJ, Grigliatti TA, Lehner CF. Genetic analysis of the *Drosophila* cdc2 homolog. Development 1993;117:219–232. [PubMed: 8223248]

47. Follette PJ, O'Farrell PH. Cdks and the *Drosophila* cell cycle. Curr Opin Genet Dev 1997;7:17–22. [PubMed: 9024630]

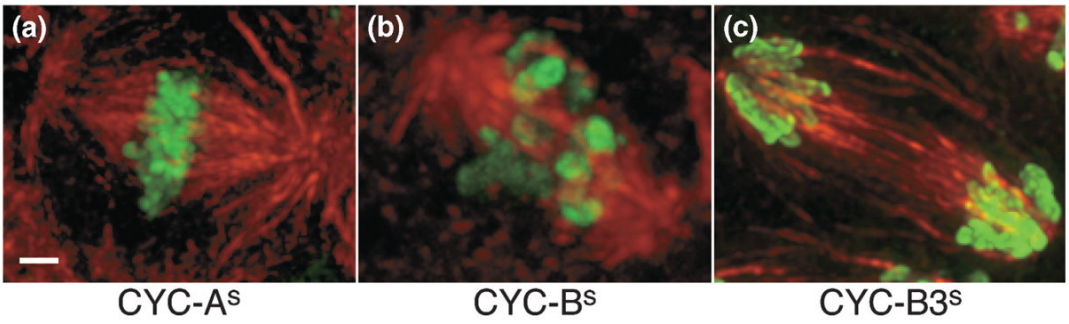

Figure 1.

Expression of stable cyclins results in distinct mitotic arrests. Indirect immunofluorescence of individual cells from fixed embryos in which the indicated stable cyclin was induced by a 30 min heat shock followed by 75 min at 25°C. Embryos were homozygous for the indicated stable cyclin transgene under the control of the heat-inducible promoter of the *Hsp70* gene. Phospho-histone H3 staining, which specifically labels mitotic chromosomes, is shown in green. β-tubulin staining of the mitotic spindle is shown in red. **(a)** Expression of CYC-A^S arrested cells in metaphase. **(b)** Expression of CYC-B^S arrested cells in a state unlike any naturally occurring stage in mitosis. Disjoined chromosomes can be seen scattered along the mitotic spindle. **(c)** Expression of CYC-B3^S arrests cells with condensed chromosomes at the poles. The scale bar indicates 1 μm.

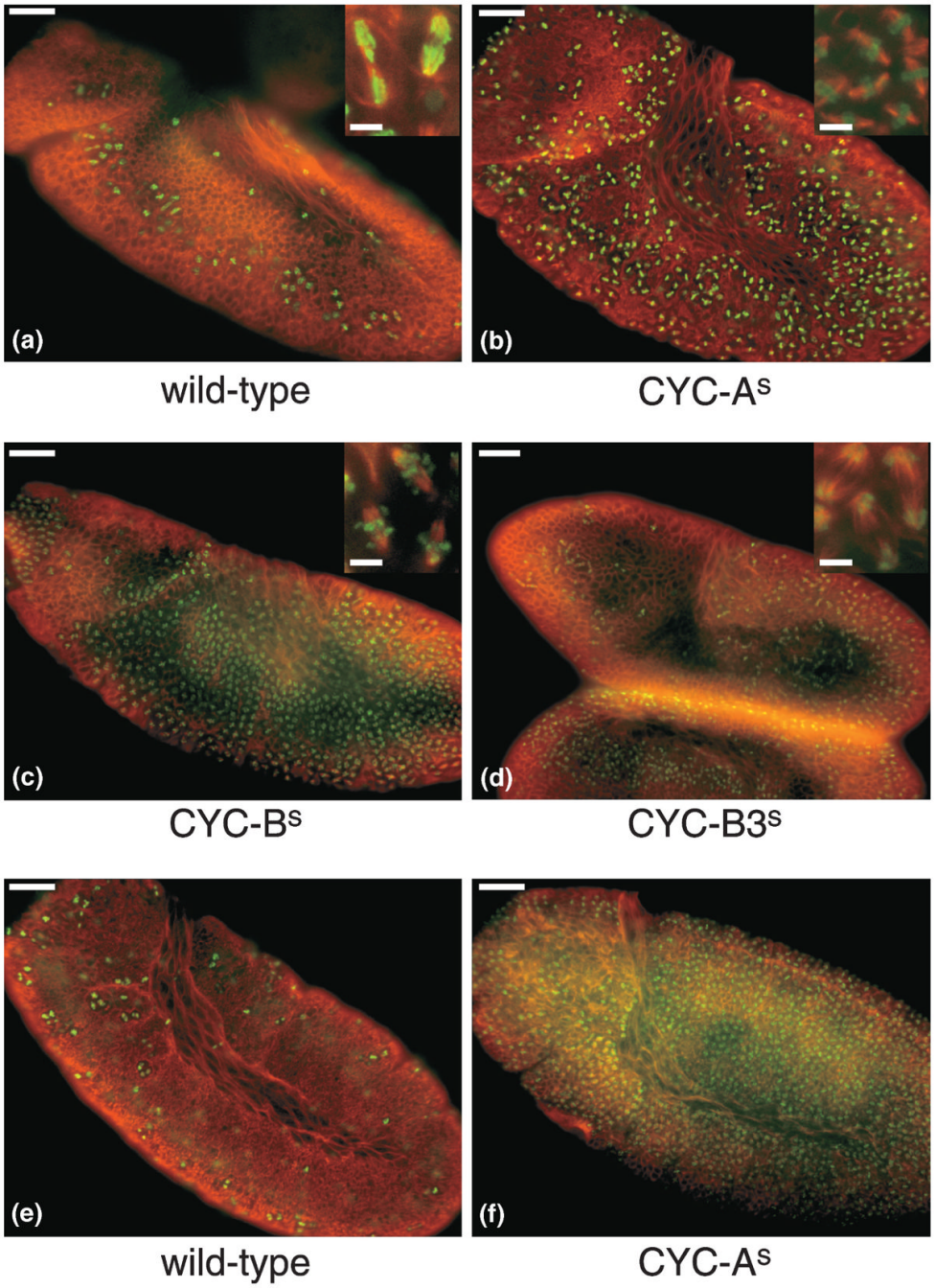

Figure 2.

Expression of stable cyclins and Cdk1 gave efficient mitotic arrest of embryos. The depicted embryos were stained for phospho-histone H3 (green) and α-tubulin (red). Insets show details of cells in the embryo. **(a)** A wild-type control embryo at a similar stage to (b–d) (stages 9 and 10). **(b)** An embryo expressing CYC-A^S and Cdk1. **(c)** An embryo expressing CYC-B^S and Cdk1. **(d)** An embryo expressing CYC-B3^S. Stable cyclin and Cdk1 expression was induced with a 30 min heat shock 165–195 min AED. Embryos were then allowed to recover for 75 min before formaldehyde fixation. **(e)** A wild-type control embryo at a similar stage to (f) (stage 11). **(f)** An embryo expressing CYC-A^S and Cdk1 showing cells arrested in cycles 15 and 16. CYC-A^S and Cdk1 expression was induced with a 30 min heat shock 300 min AED, and the

embryo was then allowed to recover for 75 min before formaldehyde fixation. The scale bars indicate 100 μm for embryo images and 5 μm for insets.

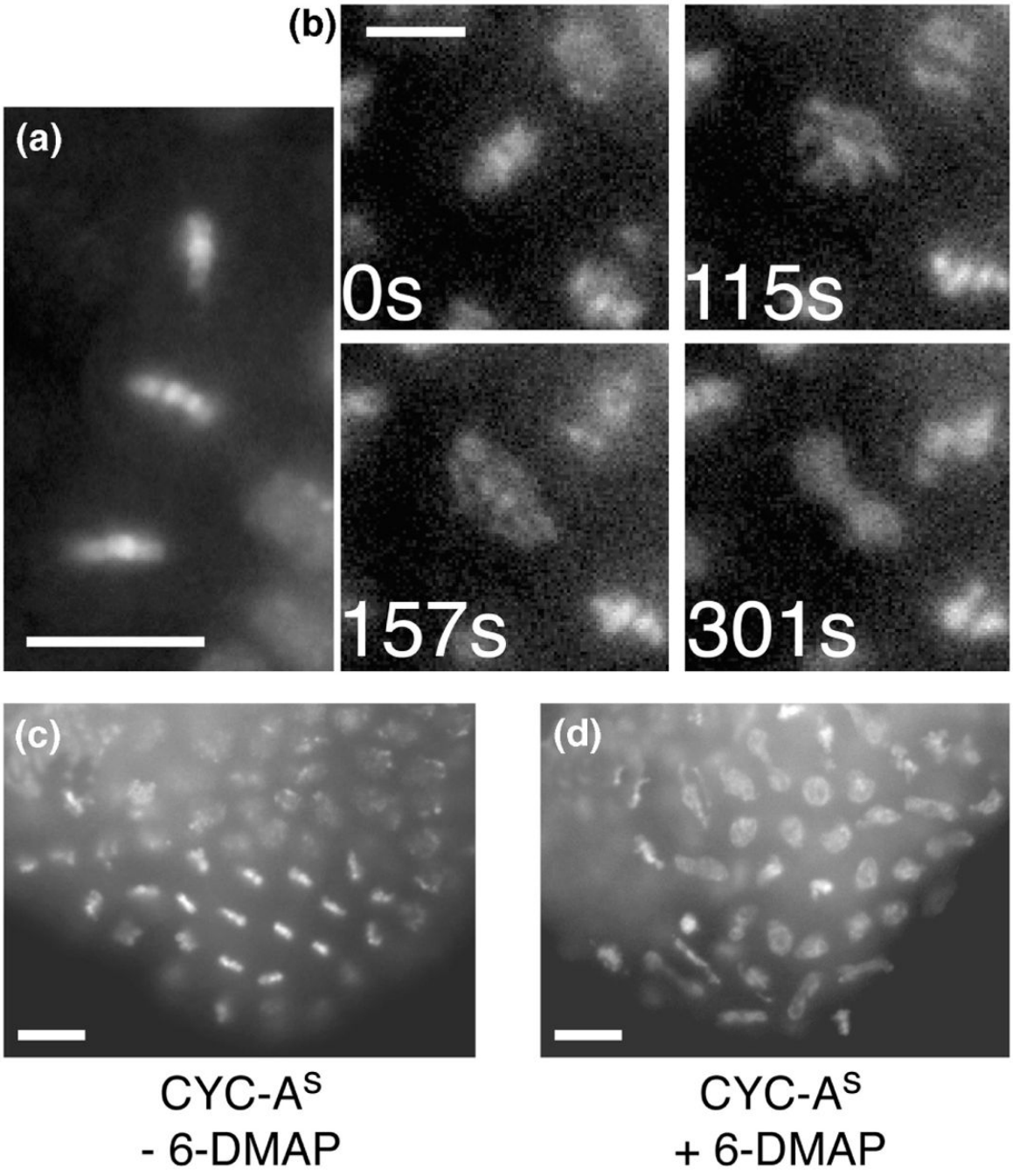

Figure 3.

Expression of CYC-A^S blocked or prolonged chromosome disjunction. Embryos homozygous for a heat shock- inducible *CYC-A*^{S} transgene and either a *histone-GFP* transgene **(a and b)** or a heat shock-inducible *Cdk1* transgene **(c and d)** were heat shocked for 30 min. (a) A single frame from Movie 1 (see supplementary material) showing the metaphase plates in three cells arrested with CYC-A^S. These cells remained in metaphase for the duration of the movie (22 min). Embryos were allowed to recover from the heat shock for ~1 hr before image acquisition began. (b) Frames from Movie 2 focusing on cell 2, which show an aberrant anaphase that followed a metaphase arrest of at least 9.5 min. Times given are in seconds from the first indication that chromosome movements disturbed the metaphase plate. In wild-type mitosis,

subsequent separation of the chromosomes is abrupt, with complete disjunction within 30 to 45 s (see Figure 4). In contrast, in this cell escaping a CYC-A^S arrest, the disjunction process was drawn out over more than 3 min and ultimately failed. The incompletely separated chromosomes decondensed and took on a "dumbbell shape" (301 s). (c and d) The tight metaphase block depends on kinase activity. Embryos were allowed to recover from the heat shock for 70 min, then were permeabilized by octane treatment, and either fixed directly with formaldehyde or soaked in Schneider's medium containing 10 mM 6-DMAP (kinase inhibitor) for 1 min before formaldehyde fixation. Fixed embryos were stained with the Hoechst DNA dye, and images were collected using a CCD. (c) Hoechst staining in an embryo not treated with 6-DMAP shows that the CYC-A^S induced metaphase block. (d) Hoechst staining in an embryo treated with 6-DMAP shows a reduction in the number of metaphase figures. In addition, several "dumbbell" figures, as described for (b), can be seen, suggesting that aberrant anaphase movements occurred. The scale bars indicate 10 μm.

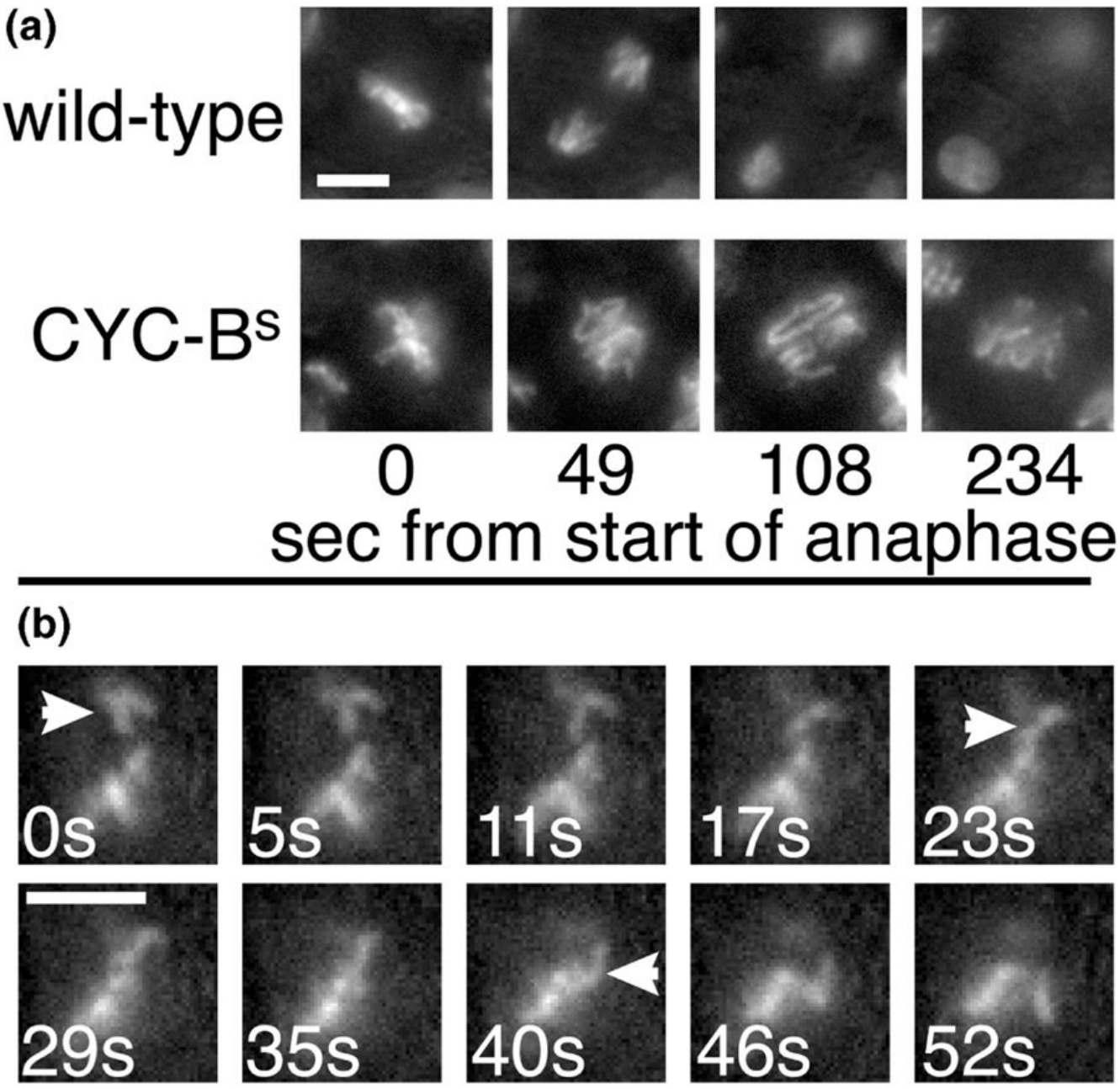

Figure 4.

(a) Anaphase progress was slowed in cells expressing CYC-B^S. A comparison of a series of time-matched frames shows that the rate and extent of chromosome movement was inhibited by the expression of CYC-B^S. In addition, at a time when the control cell had decondensed chromosomes (final frame), the CYC-B^S expressing cell was stuck in the dynamic terminal arrest state. Shown are segments of frames from Movie 3 (see supplementary material) compared to frames from a movie of a control embryo. Times given are in seconds from the first indication of anaphase movements. **(b)** Dynamic terminal arrest chromosome movements. A selected sequence of successive frames from Movie 4 illustrates the chromosome movements at the terminal arrest. The cell imaged here was arrested for at least 4.5 min when the record began. Arrows highlight a chromosome that had moved off the midline in a previous excursion

(see Movie 4), which, judging from the characteristic V shape of the chromosome, was led by the kinetochore. Over the next 35 s (7 frames), the chromosome slowly made its way back towards the midline. Given the loss of the V shape and the slow rate of these movements, we believe that this motion did not involve active pulling at the kinetochore and may indicate a loss of microtubule attachment at the kinetochore. Then, over a period of just 12 s (last 3 frames), the chromosome made a rapid movement towards the opposite pole, led by the kinetochore. Embryos homozygous for a *histone-GFP* transgene and a heat shock-inducible stable cyclin B transgene were heat shocked for 30 min and then mitosis was followed live. Control embryos were treated similarly, but lacked the stable cyclin transgene. The scale bars indicate 5μm.

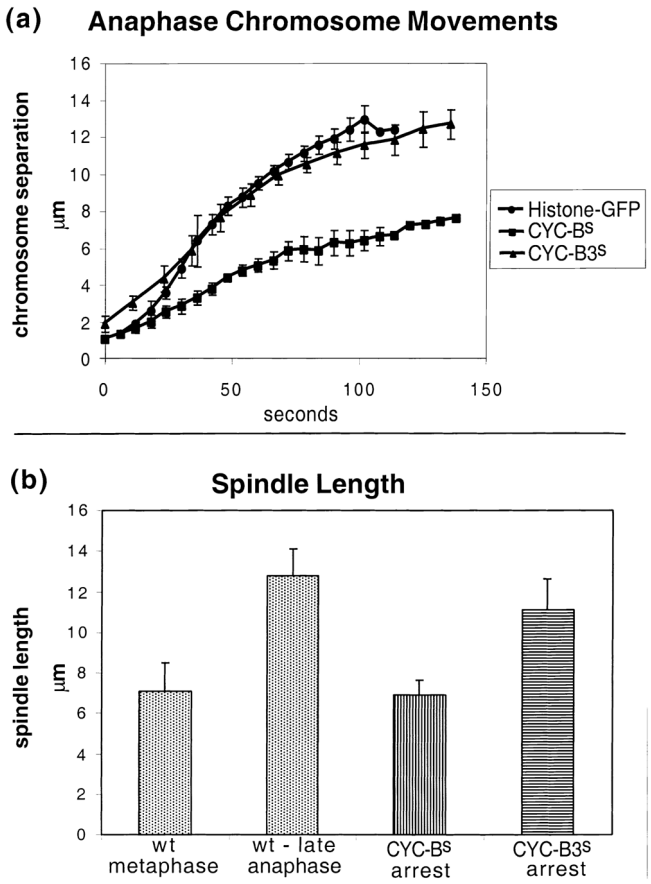

Figure 5.

Expression of CYC-B^S, but not CYC-B3^S, affects anaphase A chromosome movements and anaphase B pole separation. **(a)** Anaphase chromosome movements are slowed and never reach full separation in embryos expressing CYC-B^S but are not affected by expression of CYC-B3^S. A graph of anaphase chromosome separation with time. Data points shown are averages of multiple real-time records. The error bars indicate standard deviation. **(b)** Spindle pole separation is blocked by CYC-B^S, but not by CYC-B3^S. The spindle length of cells arrested with CYC-B^S or CYC-B3^S was compared to the spindle length of wild-type cells in metaphase or the end of anaphase. The spindle lengths were measured in fixed embryos as the distance between γ-tubulin staining dots, which mark the centrosomes. The error bars indicate standard deviation.

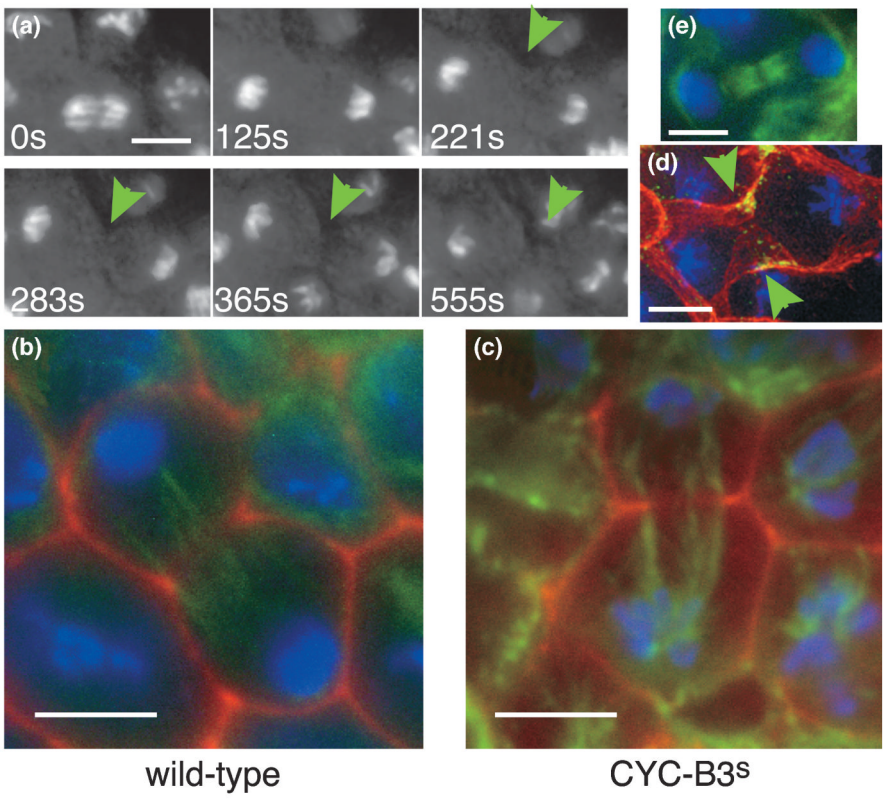

Figure 6.

Expression of CYC-B3^S results in cytokinetic furrow formation with chromosomes still condensed. **(a)** Frames from Movie 7 show visible pinching of the cell outline (arrowheads) detected with background histone-GFP fluorescence. Chromosomes remained condensed throughout the record, with individual chromosome arms visible. Embryos homozygous for a *histone-GFP* transgene and a heat shock-inducible stable cyclin B3 transgene were heat shocked for 30 min and then mitosis was followed live. Times shown are in seconds from the beginning of the movie. **(b and c)** A comparison of cytokinesis in a wild-type embryo versus an embryo expressing CYC-B3^S. After a 30 min heat shock to induce expression of CYC-B3^S, embryos were allowed to recover for one hour and were then fixed. Phalloidin staining of F-actin is shown in red, and α-tubulin staining is shown in green. Chromatin, shown in blue, was detected by phospho-histone H3 staining in (c) and Hoechst DNA staining in (b) because telophase nuclei are faint when stained for phospho-histone H3. (b) A normal cytokinetic furrow in early telophase. (c) A cell expressing CYC-B3^S shows significant cytokinetic furrow progression, while retaining condensed chromosomes and a mitotic spindle that has not developed a midbody. **(d)** Anillin staining can be seen at the cytokinetic furrow of a cell with condensed chromosomes expressing CYC-B3^S. Phospho-histone H3 staining is shown in blue, phalloidin staining of F-actin is shown in red, and anillin staining is shown in green. Arrows indicate where the plasma membrane can be seen to invaginate. The image is a projection of a three-dimensional deconvolution of stacked images taken with the DeltaVision microscopy system. **(e)** Midbody formation during cytokinesis in a wild-type embryo cell. No midbodies were seen in embryos expressing CYC-B3^S. The scale bars indicate 5 μm.

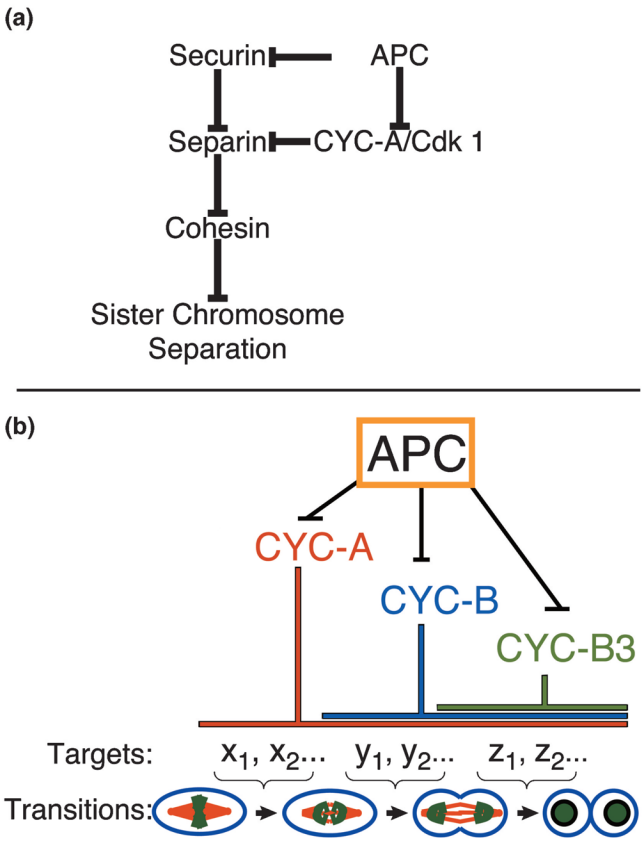

Figure 7.

Models for coupling of mitotic events to cyclin destruction. **(a)** A model for the regulation of sister chromosome separation at the metaphase/anaphase transition. The blunt arrows represent inhibition. Securins suppress a widely conserved pathway triggering sister chromosome disjunction [2]. Additionally, cyclin A and Clb5/6 act via an unknown mechanism to inhibit chromosome disjunction in *Drosophila* and *S. cerevisiae*, respectively (this report and [31]). We suggest that specific cyclin/Cdk complexes and securin act synergistically to block premature separin activity and prevent gradual cleavage of cohesin, slow loss of sister chromosome pairing, and the disruption of segregation. APC-promoted degradation of securins and cyclins at mitosis would relieve both inhibitory arms and abruptly activate separin. This model can accommodate epistasis data from both *Drosophila* and *S. cerevisiae* that are not otherwise easily reconciled [31,35]. Furthermore, careful analysis of the potency of *Drosophila* securin suggests that its function at normal levels of expression is not sufficient to block sister chromosome separation, a result that is consistent with the proposed synergistic action of securin and cyclins [35]. **(b)** Creating multiple transitions within mitosis by waves of cyclin degradation. We propose that the three mitotic cyclins, in complex with Cdk1, act to inhibit specific mitotic transitions through the phosphorylation of as yet unidentified downstream target proteins (x1, y1, etc.). In accordance with previous models, we suggest that there is an overlap in the ability of cyclins to act on downstream targets such that CYC-A/Cdk1 recognizes all of the substrates relevant to the retention of cells at metaphase, CYC-B/Cdk1 recognizes a subset of the CYC-A/Cdk1 substrates, and CYC-B3/Cdk1 recognizes a subset of the CYC-B/Cdk1 substrates [9,47]. We note that the inhibition of specific events by a particular cyclin/Cdk might be indirect and mediated by other mitotic regulators such as the Polo or Aurora kinases. As each cyclin is ubiquitinated by the APC and degraded in turn, the phosphorylation of subsets of the downstream targets can be reversed, and the inhibition of

specific mitotic transitions is relieved. In this way, the schedule of cyclin degradation coordinates events between metaphase and the return to interphase. Our data show that CYC-A^S inhibits chromosome disjunction; CYC-B^S blocks anaphase B, cytokinesis, and modifies the stability of chromosome to pole orientation; and CYC-$B3^S$ blocks numerous events that accompany the final exit from mitosis.